RSC Advances

ROYAL SOCIETY OF CHEMISTRY

www.rsc.org/advances

Graphic abstract

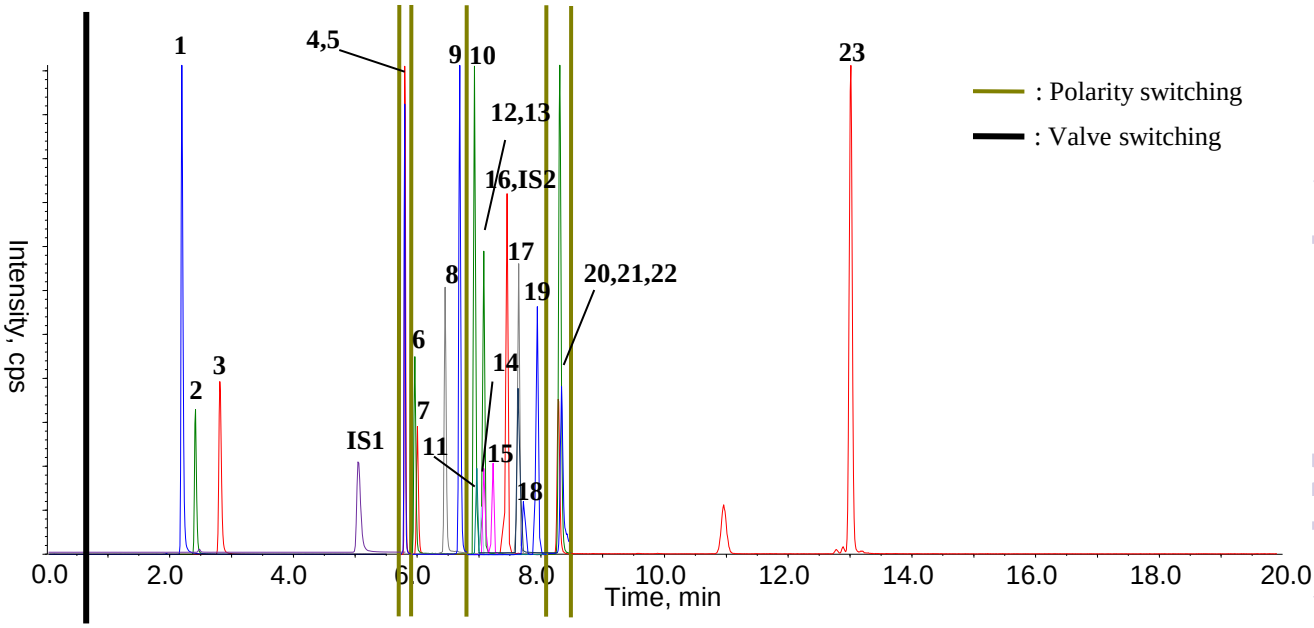

Simultaneous determination of ten aconite alkaloids and thirteen ginsenosides using online solid phase extraction hyphenated with polarity switching ultra-high performance liquid chromatography coupled with tandem mass spectrometry.

Simultaneous determination of aconite alkaloids and ginsenosides using online solid phase extraction hyphenated with polarity switching ultra-high performance liquid chromatography coupled with tandem mass spectrometry

Yuelin Song [1#], Na Zhang [1,2,3#], Yong Jiang [4], Jun Li [1], Yunfang Zhao [1], Shepo Shi [1]*, Pengfei Tu [1,4]*

[1]. *Modern Research Center for Traditional Chinese Medicine, Beijing University of Chinese Medicine, Beijing 100029, China*

[2]. *School of Chinese Materia Medica, Beijing University of Chinese Medicine, Beijing 100102, China*

[3]. *Baotou Medical College, Baotou 014060, China*

[4]. *State Key Laboratory of Natural and Biomimetic Drugs, School of Pharmaceutical Sciences, Peking University, Beijing 100191, China*

[#]: These two authors contribute equally to this article.

*Corresponding authors.

Tel./fax: +86-10-64286350; *E-mail address*: shishepo@163.com (Dr. Shepo Shi).

Tel./fax: +86-10-82802750; *E-mail address*: pengfeitu@163.com (Prof. Pengfei Tu).

ABSTRACT

Aconite alkaloids and ginsenosides have been demonstrated as the effective constituents in Shenfu injection (SFI), which is a widely used Chinese herbal formulation prepared from red ginseng and processed aconite root. Quality control is quite critical to meet the increasing demand of SFI in market and to guarantee the safety in clinic, in particular regarding those toxic aconite alkaloids. Given the significant merits of online solid phase extraction (SPE) for sample preparation, an online SPE-based method was developed to simultaneously quantify ten aconite alkaloids and thirteen ginsenosides in SFI using UHPLC–MS/MS. Because of their distinct ionization behaviors, polarity switching was implemented in ion source domain with a scheduled program, and positive and negative ionization modes were applied for alkaloids and saponins, respectively. Quantitative terms of the proposed method with respect to linearity, limit of detection, lower limit of quantification, precision, and accuracy were evaluated, and the results indicated that the method is sensitive, convenient, and reliable. The developed method was successfully applied for the simultaneous determination of aconite alkaloids and ginsenosides in ten batches of SFI (SFI1–10). The validated method can be adopted as a meaningful tool for the quality control of SFI concerning aconite alkaloids and ginsenosides, and also it offers a reliable choice for the widely qualitative analysis of constituents in complex matrices being free from tedious sample preparation procedures.

Keywords: Online solid phase extraction; Polarity switching; Aconite alkaloids; Ginsenosides; Shenfu injection.

1. Introduction

Shenfu injection (SFI) is a modern Chinese medicine preparation derived from a traditional formulation, Shenfu decoction [1]. It is prepared from the extracts of red ginseng (steamed roots of *Panax ginseng*) and aconite (processed lateral roots of *Aconitum carmichaeli*) using multistage countercurrent extraction and macroporous resin adsorption technology [2]. In comparison with the decoction, SFI is advantageous at convenience for clinical use [3]. This Chinese medicine preparation used alone or combined with other routine treatments has been widely accepted as an effective therapeutic approach for chronic congestive heart failure in clinical practices [4]. SFI has also been extensively implemented as a complementary agent for the treatment of ischemic cardiomyopathy with heart insufficiency [5], septic shock [6], acute myocardial dysfunction [7], *etc*. In addition, SFI has been suggested it is beneficial for postoperative recovery after heart surgery [8, 9] and improvement of life quality of patients undergoing chemotherapy [10-12]. In recent years, mechanism investigations have revealed that the clinical outcomes of SFI mainly rely on accelerating energy metabolism and antioxidant capacity [13, 14], modulating apoptosis [13-15], blocking sodium channels [16], inhibiting expressions of TNF-α, IL-1β, and IL-6 [17, 18], and down-regulating the activity of NF-κB [18]. As we known, aconite alkaloids and ginsenosides are the primary effective ingredients in SFI, and the modern pharmacological evaluations have demonstrated that ginsenosides offer determinant contribution for the vasodilator benefit of SFI [19], whereas the alkaloids play vital roles in cardiac electrophysiological effect for SFI by blocking ion channels [16].

Quality control is quite critical to meet the increasing demand of SFI in market and to guarantee the safety in clinic, in particular regarding those toxic aconite alkaloids. In comparison with the long history in clinical application, nonetheless, reports concerning the quality control of SFI have been seldom archived [3]. Natural variations in climate and preparation procedures usually give rise to batch-to-batch inconsistence of SFI, thus leading to safety risks, because diterpene alkaloids are of potential toxicity at the meanwhile of significant activity, even at low concentrations

[20, 21]. Therefore, it is crucial to propose sensitive and reliable analytical techniques to strictly control the concentration windows of aconite alkaloids in SFI products, as well as the ginsenosides.

Generally speaking, injection should be the isotonic solution of blood to avoid cell damage caused by the exposure of blood cells to too much or too little solute during intravenous administration; hence, it is not astonishing that our preliminary assays demonstrated a wealth of metal ions presented in SFI using inductively coupled plasma mass spectrometry (ICP-MS). As a consequence, it is critical to divert or remove those non-volatile and hydrophilic substances prior to quantitative analysis using ultra-high performance liquid chromatography hyphenated with tandem mass spectrometry (UHPLC–MS/MS), to avoid ion source contamination and signal suppression [22]. Liquid–liquid extraction (LLE) and offline solid phase extraction (SPE) generally involve tedious manual working procedures and/or relatively large amounts of solvent that must be removed prior to UHPLC–MS/MS analysis [22]; however, the superiorities of online SPE include high automatic, solvent-saving and efficiency. In view of those significant merits of online SPE for sample preparation, in current study, an online SPE-based method was developed and validated for the simultaneous determination of ten aconite alkaloids along with thirteen ginsenosides in SFI. Because of the distinct ionization properties between alkaloids and saponins, the detection of analytes was carried out by multiple reaction monitoring (MRM) scanning coupled with switching electrospray ion source polarity between positive and negative modes in a single run, and positive and negative ionization modes were applied for alkaloids and saponins, respectively.

2. Materials and method

2.1. Materials

Ginsenosides 20(*S*)-F1, 20(*S*)-F2, Rb1, Rb2, Rc, Rd, Re, Rf, Rg1, 20(*S*)-Rg3, 20(*R*)-Rh1, Ro, and pseudo-ginsenoside F11 (F11), as well as ten diterpene alkaloids, namely songorine, neoline, talatisamine, benzoylmesaconine, benzoylaconine, benzoylhypaconine, aconitine, hypaconitine, lappaconite hydrobromide, and

yunaconitine were all obtained from Shanghai Standard Biotech Co. Ltd (Shanghai, China). Their chemical structures (Fig. 1) were further elucidated in the authors' laboratory by ^{1}H-, ^{13}C-NMR and MS analyses, and the purity of each standard compound was determined to be more than 98% by normalization of the peak areas detected with HPLC–DAD–MS/MS. Two internal standards (IS), including laurotetanine (IS1, purity>98%) for aconite alkaloids and tenuifolin (IS2, purity>98%) for ginsenosides were previously purified and identified from *Litsea cubeba* and *Polygala tenuifolia* in our lab, respectively.

A total of ten batches of SFI products (SFI1–10) were all supplied by Ya'an Sanjiu Pharmaceutical Co., Ltd (Sichuan, China).

Formic acid, ammonium formate, methanol, trifluoroacetic acid (TFA), and acetonitrile (ACN) were of HPLC grade and purchased from Merck (Darmstadt, Germany). Deionized water was prepared by Milli-Q plus water purification system (Millipore, Bedford, MA, USA). The other chemicals were of analytical grade and obtained commercially from Beijing Chemical Works (Beijing, China).

2.2. Sample preparation

Stock solutions of all analytes were prepared by dissolving each authentic compound in methanol at a concentration of approximately 1.0 mg/mL and then stored at 4°C until use. Serial standard mixtures were prepared by mixing all stock solutions and subsequently diluting using Milli-Q water containing both 1.0 ng/mL of IS1 and 1.0 ng/mL of IS2 to desired concentration levels. SFI products (SFI1–10) were 1000-fold diluted with Milli-Q water spiked with IS1 and IS2 (1.0 ng/mL for either). All standard solutions and SFI samples were filtered through 0.22 μm filter membranes prior to online SPE–UHPLC–MS/MS measurement.

2.3. Online SPE–UHPLC–MS/MS analysis

The liquid chromatographic analysis was conducted on a Shimadzu UHPLC system (Shimadzu, Kyoto, Japan) consisting of two LC-20AD$_{XR}$ solvent delivery units, a LC-20AD pump, a SIL-20AC$_{XR}$ autosampler, a CTO-20AC column oven, a

SPD-M20A DAD detector, DGU-20A_{3R} degasser, and a CBM-20A controller. An ABSciex 5500 Qtrap mass spectrometer (ABSciex, Foster City, CA, USA), mounted with an electrospray ionization (ESI) interface and a 6-port/2-channel valve, was used to connect with the UHPLC system. ABSciex Analyst Software package Version 1.6.2 was adopted to synchronize the whole system, and also for data acquisition and processing. The general layout of the online SPE hyphenated with UHPLC–MS/MS instrumentation setup proposed previously was introduced in current study with minor modifications [23], and the schematic is elucidated in Fig. 2. An entire measurement was divided into two phases, the loading phase and the elution phase, by alternating the valve between A- and B-channel (Figs. 2A and 2B).

Both of the SPE column (Security Guard™, C_{18} 3.0 × 4 mm I.D., Phenomenex, Torrance, CA, USA) and the analytical column (Kinetex-C_{18} shell 4.6 × 100 mm I.D., 2.6 μm particle size, Phenomenex) were maintained at room temperature (25°C). The LC-20AD pump was responsible for delivering 2% aqueous acetonitrile containing 10 mmol/L ammonium formate to SPE column at a flow rate of 0.8 mL/min aiming to facilitate the lipophilic constituents of the injected sample being trapped in the SPE column. After flushing hydrophilic substances at loading phase (A-channel for valve) for 30 seconds (Fig. 2A), the system was switched to elution phase (B-channel for valve, Fig. 2B) and maintained for another 19.5 minutes, and the lipophilic matrix components including the analytes were back-flushed from SPE column into the analytical column using a programmed gradient condition. The mobile phase was composed of 10 mmol/L ammonium formate-H_2O (A) and 0.1% HCOOH-ACN (B) and delivered by the two LC-20AD_{XR} pumps in gradient at a flow rate of 0.8 mL/min as follows: 0–3.0 min, 20% B; 3.0–6.0 min, 20%–40% B; 6.0–10.0 min, 40% B; 10.0–15.0 min, 40%–60% B; 15.0–18.0 min, 60% B; and 18.0–20.0 min, 20% B. The temperature of autosampler was set at 4°C to stabilize samples.

The mass spectrometer was operated in MRM mode. Ion optics was tuned using standard polypropylene glycol (PPG) dilution solvent. Nitrogen was used as the nebulizer, curtain, heater, and collision gas. The ion source was heated to 500°C, and

the ion-spray voltages were maintained at 5500 V and –4500 V for positive and negative ionization, respectively. Gas setting: nebulizer gas (GS1) as 55 psi, heater (GS2) as 55 psi and curtain gas (CUR) as 35 psi. Two precursor-to-product ion transitions were recorded for each analyte or IS. The polarity-switching schedule, the precursor-to-product ion transitions, optimized declustering potential values (DP), and collision energy values (CE) are elucidated in Table 1, while the dwell time, entrance potential (EP) and collision cell exit potential (CXP) levels of each ion transition were fixed at 120 ms, 10 V, and 12 V, respectively.

The Analyst software quantification module was used to achieve the quantitative process including peak detection, peak integration, and analyte quantification. Within the automated Analyst Classic integration algorithm the smoothing factor was set as 2 and the bunching factor as 1 for all monitored peaks.

2.4. Method validation

The method validation was carried out in term of internationally accepted criterion [24].

2.4.1. Linearity, LOQ and LOD

The linearity was assayed using external calibration curves with more than seven concentration levels for each analyte, and each level was conducted in triplicate. Calibration curve generation was performed by plotting the peak area ratio of an analyte and its corresponding IS against the theoretical concentration over the calibration concentration range. A 1/x weighting function was used for the linear regression of each analyte. The acceptance criterion for each calibration curve was a correlation coefficient (r) greater than 0.99. Lower limit of quantification (LLOQ) and limit of determination (LOD) were termed as the concentration at a signal-to-noise ratio (S/N) of about 10 and 3, respectively.

2.4.2. Precision, repeatability, and stability

Intra- and inter-day variations were selected to achieve the precision assay for the proposed method. For intra-day variability evaluation, the mixed standard solutions at low, medium and high concentration levels were analyzed for six

replicates within a single day, while for inter-day assay, the solutions were examined in triplicate per day for consecutive three days. Variations were expressed by relative standard deviations (RSDs).

To evaluate the repeatability, six replicates of a selected sample (SFI1) were analyzed using the aforementioned method. The RSD value was calculated to measure the repeatability. In order to investigate the stability of the samples, the selected sample solution (SFI1) was analyzed every twelve hours within consecutive three days and the solution was stored at 4°C.

2.4.3. Recovery assay

The recovery was used to assess the accuracy of the method. Known amounts (low, medium, and high concentration levels) of mix standards solution were added into a certain amount (0.10 mL) of selected SFI (SFI1). Afterwards, the combined solution was 1000-fold diluted with Milli-Q water fortified with IS1 and IS2 (1.0 ng/mL for either) and subjected for online SPE hyphenated with UHPLC–MS/MS analysis.

3. Results and discussion

3.1. Development of online SPE–UHPLC–MS/MS

Firstly, a Phenomenex guard column was selected from several SPE columns to carry out solid phase extraction. SPE column loading procedure was modified from the method published previously [23], and the time point for valve switching was fixed before the elution of songorine by directly introducing the SPE column effluent into mass spectrometer.

Several columns were screened in term of acceptable separation for those analytes, at least between alkaloids and ginsenosides, and Phenomenex Kinetex-C_{18} shell column (100 mm × 4.6 mm i.d., particle size 2.6 μm) was finally chosen due to it is advantageous at peak capacity, peak shape, and back-pressure [25, 26], in comparison with ACE UltraCore 2.5 SuperC_{18} column (150 mm × 3.0 mm i.d., particle size 2.5 μm, Advance Chromatography Technologies Ltd., Aberdeen, Scotland), Phenomenex Kinetex-C_{18} shell column (100 mm × 2.1 mm i.d., particle

size 2.6 μm), and Capcell core ADME column (2.1 mm × 150 mm i.d., particle size 2.7 μm, Shiseido, Tokyo, Japan).

For mass parameter optimization, each analyte stock solution was diluted to appropriate content (50–100 ng/mL) by 50% aqueous methanol containing 10 mmol/L ammonium formate, and directly infused into the mass spectrometer at a rate of 10 μL/min by the syringe pump. The investigated analytes and internal standards were firstly characterized according to their MS^1 and MS^2 spectra to ascertain their precursor-to-product ion transitions for quantitative analysis. The positive and negative ionization modes were compared, and the results proved that the negative mode could provide higher responses for ginsenosides and tenuifolin (IS2), while positive ionization was found to be more suitable for aconite alkaloids and laurotetanine (IS1). After careful optimization, the formate anion-to-deprotonated ion transitions were selected for most ginsenosides, whereas positive quasi-molecular ion generated the highest responses for all alkaloids. The prominent daughter ions of alkaloids were usually yield by the neutral loss of methanol, carbon monoxide or water. Two precursor-to-product ion transitions per compound (quantifier and qualifier ion pairs) were set, with the latter one (Table 1) being matched to the quantifier ion transition in respect to CE and DP values. Ion source gas flows and ion source temperature adopted the typical ranges for the UHPLC effluent.

Finally, mobile phase modifiers were screened among ammonium acetate, formic acid, acetic acid, TFA, and ammonium formate by comparing the overall response of the analytes. Formic acid and ammonium formate were finally introduced as the modifiers for organic and aqueous mobile phases, respectively, to enhance the ionization of both ginsenosides and alkaloids.

Above all, the optimized chromatography and mass spectrometry parameters are shown in “UHPLC–MS/MS analysis” section and in Table 1.

3.2. Mass fragmentation behaviors of ginsenosides and aconite alkaloids

Aconite alkaloids and ginsenosides were widely demonstrated as the dominant

effective components in SFI. As for the bioactive ingredients in *Panax quinquefolius*, *P. notoginseng* and *P. ginseng* [27, 28], the fragmentation patterns of ginsenosides have been well defined [29, 30]. In current study, most ginsenosides generated significant intensities of $[M+HCOO]^-$ adduct ions, whereas the intensities of the expected deprotonated molecular ions ($[M-H]^-$) were relatively low due to the introduction of ammonium formate and formic acid as the mobile phase addictives (Fig. S1) [31]. When the formate anion was selected as the precursor ion to generate MS^2 spectra, neutral cleavage of formic acid (HCOOH, 46 u) occurred initially to yield the deprotonated molecular ion ($[M-H]^-$). And then, $[M-H]^-$ ion would successively expelled sugar residues, for instance glucose, rhamnose and xylose, by the dissociation of glucosidic bonds, and $[aglycone-H]^-$ (*m/z* 475 or 459) were generated finally; however, few further fragment was observed for $[aglycone-H]^-$ (Fig. S1).

On the other side, ionization and dissociation of aconite alkaloids occurred under positive ionization. Aside from songorine (C_{20}-type alkaloid), all the investigated alkaloids could be categorized into diterpene (C_{19}-type) alkaloids. It was reported that the cleavage of a methanol (CH_3OH, 32 u) moiety is the primary fragmentation pathway of aconite alkaloids [32]. When the protonated molecular ions ($[M+H]^+$) of alkaloids were transmitted to collision induce dissociation (CID) cell, the neutral losses of 32 u were usually observed attributing to the presences of methoxy groups for most alkaloids (Fig. S1). Moreover, the dissociation of H_2O was also frequently observed for C_{19}-type alkaloids. In the case of songorine, the absence of methoxy substituent resulted in the absence of 32 u loss in the MS^2 spectrum; instead, successive cleavages of H_2O (18 u) groups occurred as the prominent fragmentation pathways.

3.3. Method Validation

3.3.1. Linearity, LLOQ and LOD

A weight of 1/x was applied to minimize the relative error for the curve fitting. Correlation coefficients (r) of calibration curves in all inter-run cases were higher

than 0.99 over the concentration ranges (Table 2). The LLOQs and LODs are elucidated at Table 2. Except for ginsenosides F1, 20(*R*)-Rh1, and 20(*S*)-Rg3, the LLOQs of all analytes were lower than 20 pg/mL, and the LODs were less than 10 pg/mL. The values suggested great performances of linearity and sensitivity for the developed method.

3.3.2. Precision, repeatability and stability assays

For all targeted compounds, accuracies located at the range of 88.3−113.6% for all low, medium and high concentration levels. The RSDs of intra- and inter-day precisions were found lower than 14.9% for all analytes. Table 3 presents the results for precision assay. Those data indicated that the developed method is precise and accurate.

The repeatability presented as RSD (n = 6) was between 5.39% and 13.7%, and the results of stability assay suggested that the samples could keep stable during online SPE−UHPLC−MS/MS measurements.

3.3.3. Recovery assay

Known amounts (low, medium and high concentration levels) of mix standards solution were added into 0.10 mL of SFI product (SFI1) prior to online SPE−UHPLC−MS/MS analysis. The recoveries were observed between 86.1% and 112.9% for all analytes, which could satisfy the quantitative criteria for alkaloids and ginsenosides in complex matrices (Table 3).

In addition, the impacts from carryover and re-injection were also assessed and the results suggested that influences of these two items could be neglected due to the quite slight influence of them.

3.4. Determination of twenty-three analytes in SFI

The developed online SPE−UHPLC−MS/MS system was applied for simultaneous quantification of twenty-three analytes in ten batches of SFI products (SFI1−10). The typical chromatogram of SFI is shown in Fig. 3B, and all the determined contents are summarized in Table 4.

Overall, the contents of ginsenosides were much higher than those of aconite

alkaloids, which are in great coincidence with the findings archived in Ref. [3, 33]; however, ginsenoside 20(*S*)-F1 and pseudo-ginsenoside F11 were not detected in all SFI samples. In particular, ginsenosides Rb1, Rg1, Rc, Rb2, Re, and 20(*S*)-Rg3 were determined as the abundant constituents, whereas the contents of ginsenosides Rd and 20(*R*)-Rh1 were slightly lower than the other ginsenosides. Although the toxicity of aconite alkaloids was widely mentioned, the contents of those compounds in SFI (lower than 1.0 μg/mL for most alkaloids) ascertained the location at the safety window with a clinical dosage. In particular, trace distributions (lower than 0.1 μg/mL in most cases) were revealed for aconitine, yunaconitine, and hypaconitine, particularly lappaconite hydrobromide, which are sorted into diester-diterpenoid alkaloids and exhibit greater toxic possibility than those monoester-diterpenoid alkaloids [34]. The contents of both ginsenosides and aconite alkaloids showed relatively big variations (approximately 3 folds) among different batches.

In practice, a problem for the hyphenation of LC and MS is that nonvolatile substances cannot be introduced into the mass spectrometer, since the nonvolatile salts, particularly metal ions, dramatically degrade its performance [35−37]. In addition, the metals can also join with analytes having carboxyl, carbonyl, ether or ester group to form cluster adducts, which could result in irreproducible quantitative results. We preliminarily measured the contents of metals in SFI using Elan DRCII ICP-MS (Perkin Elmer, Waltham, MA, USA). The contents of Na^+, and K^+ were measured as 628.0 and 62.6 μg/mL in SFI, respectively, and the total contents of some other metals, such as Fe, Mg, and Ca, were determined more than 4 μg/mL. Therefore, when SFI was directly injected into mass spectrometer, it is of a great risk for contaminating our system. We were reluctant to risk contaminating our system, which is used for many other purposes; thus, we did not have the opportunity to obtain information about the long-term influence of metal ions on mass spectrometer performance.

Despite that a couple of methods have been proposed to monitor ginsenosides and aconite alkaloids in Shenfu products using UHPLC–MS/MS, our current study is advantageous at synchronous determination, pretreatment-free and high sensitivity.

Further studies are ongoing in our laboratory on characterization of the pharmacokinetic profiles of SFI in rats, and the proposed online SPE−UHPLC−MS/MS system is expected to be an appropriate technique to directly analyze the biological samples.

4. Concluding remarks

A novel sensitive and selective online SPE hyphenated with UHPLC–MS/MS method operating negative and positive switching mode in a single analysis process was developed and validated in terms of LOD, LLOQ, linearity, precision, accuracy and recovery assays. A total of twenty-three constituents, including ten aconite alkaloids and thirteen ginsenosides, were simultaneously determine in ten batches of SFI. Above all, the validated method not only provides a meaningful tool for the quality control of SFI, but also offers a reliable choice for the widely qualitative analysis of constituents in complex matrices without tedious sample preparation procedures.

Acknowledgement

This work was financially supported by National Key Technology R&D Program "New Drug Innovation" of China (Nos. 2013ZX09201018, 2012ZX09103201-036 and 2012ZX09301002-002-002), and the National Natural Science Foundation of China (No. 81403073).

Appendix Supplementary data

Supplementary data (Supplemental figures) associated with this article can be found, in the online version, at http://dx.doi.org/.....

References

[1] Z. Li, R. Zhang, X. Wang, X. Hu, Y. Chen, and Q. Liu, *Biomed. Chromatogr.*, in press. DOI: 10.1002/bmc.3272.

[2] Q. Zhang, and C. Li, *Evid. Based Complement. Alternat. Med.*, **2013**, 319092.

[3] H. Yang, L. Liu, W. Gao, K. Liu, L.W. Qi, and P. Li, *J. Pharm. Biomed. Anal.*, 2014, **92**, 13–21.

[4] W.T. Song, F.F. Cheng, X. Li, C.R. Lin, and J.X. Liu, *Evid. Based Complement. Alternat. Med.*, **2012**, 713149.

[5] X.Y. Luo, F.R. Zhang, and R.M. He, *Chin. J. Integr. Med.*, 2009, **29**, 685–687.

[6] J. Hu, Z.Y. Fu, Y.M. Xie, J. Wang, W.W. Wang, and X. Liao, *Zhongguo Zhong Yao Za Zhi*, 2013, **38**, 3209–3214.

[7] Z.E. Li, *Chin. J. Integr. Med.*, 2006, **26**, 555–557.

[8] C.D. Zheng, and S. Min, Chin. *J. Integr. Med.*, 2008, **14**, 10–16.

[9] H. Dong, L.Z. Xiong, and M. Chen, *Chin. J. Integr. Med.*, 2004, **24**, 32–35.

[10] W.Y. Wu, S.Q. Long, H.B. Zhang, X.S. Chai, H. Deng, X. G. Xue, B. Wang, H.Y. Luo, and W.S. Liu, *Chin. J. Integr. Med.*, 2006, **12**, 50–54.

[11] W.Y. Wu, S.Q. Long, and X.S. Chai, *Chin. J. Integr. Med.*, 2009, **29**, 19–22.

[12] S.Q. Long, G.Y. Liao, W. F. He, B. Wang, H. Deng, H.B. Zhang, X.S. Chai, J.Z. Cai, and W.Y. Wu, *Nan Fang Yi Ke Da Xue Xue Bao*, 2011, **31**, 2090–2092.

[13] M.Y. Zhang, X.F. Ji, S. Wang, and C.S. Li, *Resuscitation*, 2012, **83**, 1152–1158.

[14] X.F. Ji, L. Yang, M.Y. Zhang, C.S. Li, S. Wang, and L.H. Cong, *Shock*, 2011, **35**, 530–536.

[15] W. Gu, C. Li, W. Yin, Z. Guo, X. Hou, and D. Zhang, *Shock*, 2012, **38**, 301–306.

[16] J. Luo, S.K. Min, K. Wei, J. Cao, *J. Ethnopharmacol.*, 2008, **117**, 439–445.

[17] D.Z. Ke, Q.W. Chen, C.L. Li, and G.Q. Li, *Zhongguo Zhong Yao Za Zhi*, 2007, **32**, 2273–2277.

[18] J. Wang, L.F. Qiao, and G.T. Yang, *Chin. J. Integr. Med.*, 2008, **14**, 51–55.

[19] J. Zhu, L. Kang, Q. Ye, G. Fan, Y. Liang, C. Yan, and J. Orgah, *PloS one*, 2013, **8**, e78026.

[20] X. Wang, H. Wang, A. Zhang, X. Lu, H. Sun, H. Dong, and P. Wang, *J. Proteome Res.*, 2012, **11**, 1284–1301.

[21] L. Ye, T. Wang, C. Yang, L. Tang, J. Zhou, C. Lv, Y. Gong, Z. Jiang, and Z. Liu, *Toxicol. Lett.*, 2011, **204**, 81–91.

409 [22] Y.L. Song, W.H. Jing, R. Yan, and Y.T. Wang, *Anal. Methods*, 2014, **6**, 623–628.
410 [23] Y.L. Song, W.H. Jing, F.Q. Yang, Z. Shi, M.C. Yao, R. Yan, and Y.T. Wang, *J.*
411 *Pharm. Biomed. Anal.*, 2014, **88**, 269–277.
412 [24] U.S. Food and Drug Administration, Bioanalytical method validation, in:
413 Guidance for Industry, U.S. Food and Drug Administration, 2001, p. 1.
414 [25] G. Du, H. Zhao, Y. Song, Q. Zhang, and Y. Wang, *J. Sep. Sci.*, 2011, **34**, 2576–
415 2585.
416 [26] Y.L. Song, W.H. Jing, G. Du, F.Q. Yang, R. Yan, and Y.T. Wang, *J. Chromatogr.*
417 *A*, 2014, **1338**, 24–37.
418 [27] W.Z. Yang, Y. Hu, W.Y. Wu, M. Ye, and D.A. Guo, *Phytochemistry*, 2014, **106**,
419 7–24.
420 [28] L.W. Qi, C.Z. Wang, and C.S. Yuan, *Nat. Prod. Rep.*, 2011, **28**, 467–495.
421 [29] W.Z. Yang, M. Ye, X. Qiao, C. F. Liu, W.J. Miao, T. Bo, H.Y. Tao, and D.A.
422 Guo, *Ana. Chim. Acta*, 2012, **739**, 56–66.
423 [30] L.W. Qi, H.Y. Wang, H. Zhang, C.Z. Wang, P. Li, and C.S. Yuan, *J. Chromatogr.*
424 *A*, 2012, **1230**, 93–99.
425 [31] E.C. Chan, S.L. Yap, A.J. Lau, P.C. Leow, D.F. Toh, and H.L. Koh, *Rapid*
426 *Commun. Mass Spectrom.*, 2007, **21**, 519–528.
427 [32] J. Zhang, Z.H. Huang, X.H. Qiu, Y.M. Yang, D.Y. Zhu, and W. Xu, *PloS one*,
428 2012, **7**, e52352.
429 [33] N. Guo, M. Liu, D. Yang, Y. Huang, X. Niu, R. Wu, Y. Liu, G. Ma, and D. Dou,
430 *Chem. Cent. J.*, 2013, **7**, 165.
431 [34] Y.F. Zhao, F.R. Song, H. Yue, X.H. Guo, H.L. Li, Z. Q. Liu, and S.Y. Liu, *Chem.*
432 *J. Chin. U.*, 2007, **28**, 2051–2055.
433 [35] H. Yoshida, T. Mizukoshi, K. Hirayama, and H. Miyano, *J. Chromatogr. A.*,
434 2006, **1119**, 315–321.
435 [36] U. Sommer, H. Herscovitz, F.K. Welty, and C.E. Costello, *J. Lipid Res.*, 2006,
436 **47**, 804–814.
437 [37] H. Yoshida, T. Mizukoshi, K. Hirayama, and H. Miyano, *J. Agric. Food Chem.*,
438 2007, **55**, 551–560.

439

Figure legends

Fig. 1 Chemical structures and molecular weights (M.W.) of and 23 analytes investigated in this study, including thirteen ginsenosides, 20(*S*)-F1, 20(*S*)-F2, Rb1, Rb2, Rc, Rd, Re, Rf, Rg1, 20(*S*)-Rg3, 20(*R*)-Rh1, Ro, and pseudo-ginsenoside F11 (F11), as well as ten diterpene alkaloids, songorine, neoline, talatisamine, benzoylmesaconine, benzoylaconine, benzoylhypaconine, aconitine, hypaconitine, lappaconite hydrobromide, and yunaconitine.

Fig. 2 Connectivity sketch of the six-port switching valve controlling the online SPE hyphenated with UHPLC–MS/MS step. Loading phase: the specimen aliquot delivered from the auto-sampler is captured onto the SPE column using 2% aqueous acetonitrile containing 10 mM ammonium formate to expel those hydrophilic and non-volatile substances, for example metal ions, while the valve is maintained at A-channel; elution phase: the specimen fraction adsorbed onto the SPE column, mainly containing ginsenosides, aconite alkaloids, and some other apolar substances, is eluted using a programmed gradient elution and subsequent to MS/MS detection, and the valve is maintained at B-channel. Details are described at Section 2.3. Online SPE–UHPLC–MS/MS analysis.

Fig. 3 Representative multiple ion pairs extracted ion current (TIC) chromatograms of MRM mode of reference compounds mixture (A) and SFI product (SFI1, B). As described above, valve switching (marked with black line) occurs at 0.5 min, and polarity switching (marked with brown line) occurs for five times. Except for loading phase (0–0.5 min), each segment is magnified to make every signal visible, and the intensities of all the base peaks (highest signals) are elucidated. **1**, Songorine; **2**, Neoline; **3**, Talatisamine; **4**, Rg1; **5**, Re; **6**, Benzoylmesaconine; **7**, Lappaconite hydrobromide; **8**, Benzoylaconine; **9**, Benzoylhypaconine; **10**, F11; **11**, Rb1; **12**, Ro; **13**, Rf; **14**, Rc; **15**, Rb2; **16**, 20(*S*)-Rg2; **17**, Rd; **18**, 20(*R*)-Rh1; **19**, 20(*S*)-F1; **20**, Aconitine; **21**, Yunaconitine; **22**, Hypaconitine; **23**, 20(*S*)-Rg3.

Table 1 The precursor-to-product ion transitions, declustering potential values (DP), collision energy values (CE), retention times (t_R) of the 23 targeted components and t the polarity switching schedule.

period	duration	analyte	t_R (min)	Ion transition Precursor>product[a]	DP (V)	CE (eV)
period 1 (positive)	5.70	Songorine	2.24	**358>340**; 358>322	100	39
		Neoline	2.46	**438>420**; 438>388	120	40
		Talatisamine	2.88	**422>390**; 422>358	120	39
		IS1	4.94	**328>311**; 328>280	100	17
period 2 (negative)	0.17	Rg1	5.78	**845>845**;845>799	-100	-11
		Re	5.78	**991>991**;991>945	-100	-11
period 3 (positive)	0.93	Benzoylmesaconine	5.95	**590>540**; 590>558	90	48
		Lappaconite hydrobromide	5.99	**585>356**; 585>324	60	46
		Benzoylaconine	6.44	**604>554**; 604>572	100	47
		Benzoylhypaconine	6.67	**574>542**; 547>510	103	47
period 4 (negative)	1.31	F11	6.91	**845>845**;845>799	-100	-11
		Rb1	6.95	**1153>1153**;1153>1107	-100	-15
		Ro	7.02	**1001>1001**;1001>955	-100	-15
		Rf	7.06	**845>845**;845>799	-100	-11
		Rc	7.06	**1123>1123**;1123>1077	-100	-15
		Rb2	7.20	**1123>1123**; 1123>1077	-100	-15
		20(*S*)-Rg2	7.42	**829>829**;829>783	-100	-11
		IS2	7.44	**679>679**;679>455	-100	-15
		Rd	7.61	**991>991**;991>945	-100	-15
		20(*R*)-Rh1	7.69	**683>683**;683>637	-100	-11
		20(*S*)-F1	7.90	**683>683**;683>637	-100	-11
period 5 (positive)	0.40	Aconitine	8.28	**646>586**; 646>526	120	44
		Yunaconitine	8.31	**660>600**; 660>568	107	42
		Hypaconitine	8.34	**616>556**; 616>524	130	44
period 6 (negative)	11.49	20(*S*)- Rg3	13.03	**829>829**;829>783	-100	-11

[a]: two ion pairs were optimized for each analyte, and the ion transitions in bold were adopted for quantitative analysis, while the other one was adopted as qualifier ion pair.

474 **Table 2** Linear regression data, lower limits of quantification (LLOQs) and limits of
475 detection (LODs) for all targeted analytes.

Analyte	Linear regression data			LLOQ	LOD
	Regression equation	r	Linear range (ng/mL)	(pg/mL)	(pg/mL)
Songorine	y = 17.1 x – 0.341	0.997	0.0816–20.4	6.53	1.31
Neoline	y = 3.3 x + 0.265	0.999	0.0190–59.5	7.62	1.52
Talatisamine	y = 5.06 x – 0.165	0.999	0.0176 – 55.0	7.04	1.41
Rg1	y = 1.4 x + 3.61	0.996	0.476 – 119.0	7.62	1.52
Re	y = 0.542 x + 1.44	0.999	0.0282 – 88.0	5.63	1.13
Benzoylmesaconine	y = 1.79 x + 0.129	0.997	0.0712 – 44.5	0.11	0.06
Lappaconite hydrobromide	y = 1.82 x – 0.0461	0.997	0.0728 – 45.5	1.16	0.58
Benzoylaconine	y = 2.64 x – 0.000127	0.999	0.0848 – 53.0	1.36	0.68
Benzoylhypaconine	y = 3.89 x + 0.302	0.999	0.0310 – 48.5	1.24	0.62
F11	y = 0.607 x + 0.113	0.997	0.336 – 84.0	5.38	1.08
Rb1	y = 0.17 x + 0.0853	0.990	0.195 – 122	7.81	1.56
Ro	y = 0.818 x +0.438	0.998	0.128 – 80.0	2.56	1.02
Rf	y = 0.387 x + 0.425	0.997	0.340 – 85.0	5.44	2.72
Rc	y = 0.0625 x + 0.0449	0.996	0.0291 – 91.0	5.82	2.91
Rb2	y = 0.0603 x + 0.0731	0.990	0.0397 – 124	7.94	3.97
20(*S*)–Rg2	y = 0.467 x + 1.12	0.991	0.252 – 63.0	4.03	2.02
Rd	y = 0.226 x + 0.324	0.997	0.0784 – 98.0	6.27	3.14
20(*R*)–Rh1	y = 1.67 x – 0.00622	0.999	0.656 – 82.0	78.4	15.7
20(*S*)–F1	y = 1.48 x + 0.0355	0.999	0.157 – 98.0	392	157
Aconitine	y = 1.95 x – 0.13	0.996	0.0888 – 55.5	17.8	7.10
Yunaconitine	y = 4.34 x – 0.17	0.998	0.0944 – 59.0	18.9	7.55
Hypaconitine	y = 2.17 x + 0.127	0.996	0.0776 – 48.5	15.5	6.21
20(*S*)–Rg3	y = 0.0997 x + 0.175	0.993	0.108 – 67.5	108.0	54.0

476 **Table 3** Intra-, inter-day and recovery performance parameters of quality control
477 samples for all monitored analytes (n = 6).

Analyte	Concentration (ng/mL)	Intra-day RSD (%)	Inter-day RSD (%)	Recovery (%)	RSD (%)
Songorine	low	3.76	12.3	97.9	4.31
	medium	8.05	4.53	93.2	3.24
	high	13.2	14.8	91.3	1.93
Neoline	low	8.31	14.4	95.5	2.17
	medium	7.69	3.06	96.1	2.64
	high	14.6	14.7	108.6	1.98
Talatisamine	low	5.91	11.5	96.8	3.33
	medium	7.43	4.08	103.4	4.12
	high	13.3	14.9	111.1	1.44
Rg1	low	9.73	11.8	106.6	9.87
	medium	11.3	13.5	109.2	10.2
	high	10.6	12.4	95.8	8.94
Re	low	10.7	12.5	97.1	9.25
	medium	12.3	13.6	99.3	9.88
	high	11.8	13.9	100.4	11.0
Benzoylmesaconine	low	9.58	9.08	96.8	2.40
	medium	7.33	5.08	101.2	1.35
	high	13.6	14.9	106.4	3.54
Lappaconite hydrobromide	low	5.45	10.6	98.3	4.56
	medium	7.55	4.48	97.9	1.97
	high	12.8	13.9	108.8	3.61
Benzoylaconine	low	6.09	11.9	99.6	1.88
	medium	8.46	5.83	98.9	1.43
	high	13.1	13.9	102.4	3.65
Benzoylhypaconine	low	6.44	9.62	103.1	1.49
	medium	6.78	3.70	101.7	5.23
	high	13.7	14.5	98.5	3.44
Rb1	low	12.1	13.9	86.1	8.95
	medium	9.80	11.7	89.9	9.13
	high	13.9	14.1	111.2	9.23
Ro	low	8.52	11.6	90.1	10.4
	medium	7.83	13.3	113.2	9.67
	high	11.6	14.6	98.5	8.91
Rf	low	11.1	12.9	101.7	10.3
	medium	10.4	13.1	111.6	11.1
	high	10.9	9.97	95.4	7.99
Rc	low	9.01	10.0	89.9	10.4
	medium	9.53	8.13	92.2	11.3
	high	11.3	7.46	98.8	10.6

Rb2	low	7.84	11.3	112.9	8.93
	medium	6.53	9.37	107.1	10.5
	high	8.10	10.8	96.0	11.4
20(*S*)-Rg2	low	6.54	9.03	112.7	10.3
	medium	7.27	6.55	107.5	9.86
	high	8.43	10.9	110.9	10.6
Rd	low	9.35	14.0	95.5	9.65
	medium	10.3	12.8	93.1	9.73
	high	8.24	10.6	91.3	9.32
20(*R*)-Rh1	low	9.17	12.5	97.2	10.8
	medium	9.20	11.1	109.4	9.98
	high	11.3	12.4	108.8	10.0
Aconitine	low	5.19	2.34	98.4	3.21
	medium	7.59	2.59	99.1	4.36
	high	12.63	12.41	96.5	2.95
Yunaconitine	low	5.16	2.74	97.2	3.71
	medium	8.36	3.68	104.2	5.23
	high	12.65	12.62	106.6	4.51
Hypaconitine	low	10.32	7.22	102.3	2.55
	medium	9.28	3.36	95.8	1.98
	high	12.53	13.82	98.9	3.72
20(*S*)-Rg3	low	7.37	8.77	111.2	11.4
	medium	8.46	9.13	109.9	10.8
	high	11.4	13.2	91.1	10.0

478

479 **Table 4** The contents (μg/mL) of investigated compounds in the ten batches of Shenfu injection (SFI1–10)

Samples	Contents																				
	1[a]	**2**	**3**	**4**	**5**	**6**	**7**	**8**	**9**	**11**	**12**	**13**	**14**	**15**	**16**	**17**	**18**	**20**	**21**	**22**	**23**
SF1	0.162± 0.02	0.646± 0.08	0.103± 0.01	135.3± 14.9	74.2± 7.02	1.76± 0.22	0.026± 0.00	0.174± 0.02	0.528± 0.08	191.2± 44.7	69.0± 10.3	91.2± 13.8	48.7±5 .73	76.0± 14.6	34.2± 5.64	37.4± 3.12	35.8± 3.72	0.070± 0.00	0.041± 0.00	0.027± 0.01	74.9± 12.8
SF2	0.145± 0.04	0.601± 0.22	0.094± 0.05	150.4± 9.38	81.7± 4.9	1.23± 0.40	0.026± 0.00	0.130± 0.05	0.323± 0.13	245.6± 31.2	51.8± 8.17	63.0± 4.06	114.4± 11.0	80.8± 12.4	32.5± 6.69	27.4± 2.34	36.0± 4.40	0.072± 0.00	0.041± 0.00	0.042± 0.03	65.4± 5.14
SF3	0.116± 0.01	0.487± 0.05	0.066± 0.01	130.0± 16.9	75.6± 14.7	0.90± 0.14	0.026± 0.00	0.114± 0.02	0.411± 0.07	154.3± 25.9	40.6± 8.02	72.0± 6.40	79.7±1 0.9	49.0± 7.16	40.2± 3.34	31.4± 5.33	37.2± 6.74	0.070± 0.00	0.040± 0.00	0.029± 0.03	73.7± 12.5
SF4	0.219± 0.08	0.919± 0.38	0.158± 0.07	107.6± 7.91	67.7± 7.42	1.60± 0.56	0.027± 0.00	0.209± 0.08	0.709± 0.29	136.6± 25.9	29.2± 4.10	55.2± 6.98	86.2±9 .24	47.8± 6.63	49.6± 5.28	38.6± 3.02	36.6± 1.36	0.072± 0.00	0.041± 0.00	0.053± 0.04	49.6± 4.94
SF5	0.192± 0.06	0.776± 0.30	0.134± 0.07	122.8± 6.68	74.3± 8.28	1.37± 0.47	0.028± 0.00	0.179± 0.06	0.611± 0.24	137.5± 26.3	32.0± 5.60	54.4± 5.26	94.2±1 2.2	46.1± 6.17	55.8± 4.48	42.8± 5.44	37.2± 2.90	0.075± 0.01	0.044± 0.01	0.033± 0.03	56.4± 8.76
SF6	0.188± 0.05	0.730± 0.22	0.123± 0.05	132.3± 22.0	84.1± 15.7	2.05± 0.70	0.027± 0.00	0.233± 0.07	0.856± 0.29	79.3±1 1.1	24.0± 2.6	82.8± 4.90	46.3±7 .93	26.4± 1.59	39.7± 4.42	28.8± 3.86	30.6± 5.18	0.073± 0.00	0.043± 0.00	0.060± 0.03	29.6± 2.90
SF7	0.267± 0.02	1.23±0 .08	0.272± 0.03	128.6± 17.8	79.6± 16.8	2.48± 0.20	0.027± 0.00	0.317± 0.03	1.11±0. 11	137.8± 19.9	34.8± 1.44	90.8± 8.43	65.8±1 8.4	64.7± 3.66	40.3± 7.51	46.8± 3.09	35.4± 4.98	0.076± 0.00	0.041± 0.00	0.093± 0.02	75.2± 10.3
SF8	0.148± 0.02	0.817± 0.19	0.160± 0.03	116.0± 14.3	57.6± 8.99	0.74± 0.13	0.027± 0.00	0.108± 0.02	0.278± 0.04	89.8±1 4.5	23.6± 4.64	77.0± 8.90	44.0±8 .17	45.8± 5.41	24.2± 4.64	25.8± 2.20	26.2± 1.04	0.078± 0.00	0.042± 0.00	0.104± 0.03	36.9± 3.76
SF9	0.249± 0.08	0.663± 0.05	0.215± 0.02	146.9± 11.7	83.4± 10.2	1.74± 1.13	0.031± 0.00	0.213± 0.08	0.545± 0.30	193.5± 20.1	37.0± 1.38	67.4± 8.97	99.8±1 8.3	59.3± 7.13	43.4± 3.11	47.4± 6.74	38.6± 7.60	0.165± 0.06	0.051± 0.00	0.692± 0.51	48.2± 6.39
SF10	0.112± 0.03	0.490± 0.12	0.117± 0.05	121.2± 12.7	78.4± 9.51	0.49± 0.45	0.038± 0.01	0.080± 0.05	0.161± 0.13	169.9± 25.5	47.2± 5.5	50.0± 7.08	95.5±1 0.1	55.5± 8.31	38.0± 6.14	31.2± 4.76	32.8± 5.22	0.091± 0.03	0.058± 0.02	0.094± 0.10	56.4± 6.01

[a]: **1**, Songorine; **2**, Neoline; **3**, Talatisamine; **4**, Rg1; **5**, Re; **6**, Benzoylmesaconine; **7**, Lappaconite hydrobromide; **8**, Benzoylaconine; **9**, Benzoylhypaconine; **11**, Rb1; **12**, Ro; **13**, Rf; **14**, Rc; **15**, Rb2; **16**, 20(*S*)–Rg2; **17**, Rd; **18**, 20(*R*)–Rh1; **20**, Aconitine; **21**, Yunaconitine; **22**, Hypaconitine; **23**, 20(*S*)–Rg3.

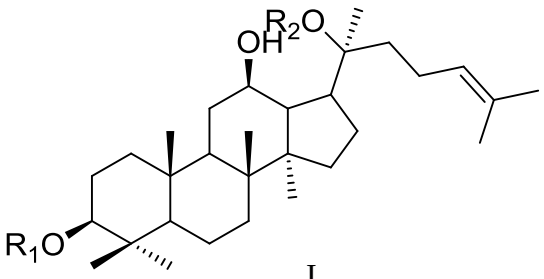

I

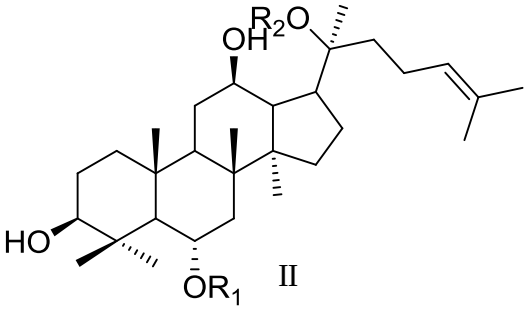

II

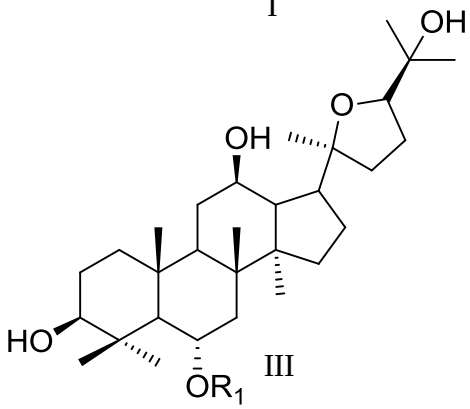

III

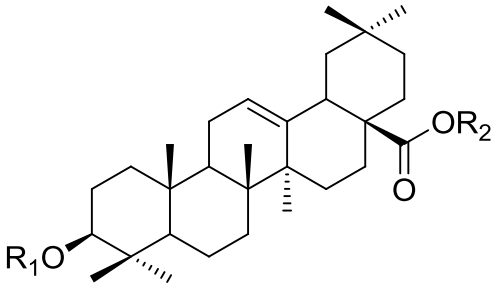

IV

Compound	Skeleton	R_1	R_2	M.W.
Rb1	I	glc(2-1)glc	glc(4-1)glc	1108
Rb2	I	glc(2-1)glc	glc(4-1)ara	1078
Rc	I	glc(2-1)glc	glc(6-1)ara	1078
Rd	I	glc(2-1)glc	glc	946
20(*S*)-Rg3	I	glc(2-1)glc	H	784
20(*S*)-Rg2	II	glc(2-1)rha	H	784
20(*S*)-F1	II	H	glc	638
Re	II	glc(2-1)rha	glc	946
Rf	II	glc(2-1)glc	H	800
Rg1	II	glc	glc	800
20(*R*)-Rh1	II	glc	H	638
F11	III	glc(2-1)rha	-	800
Ro	IV	gluA(2-1)glc	glc	956

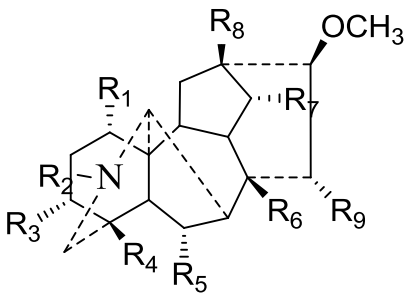

Skeleton of alkaloids

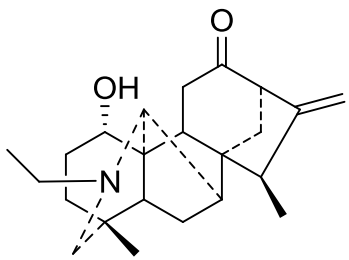

Songorine (M.W.: 357)

Compound	R_1	R_2	R_3	R_4	R_5	R_6	R_7	R_8	R_9	M.W.
Aconitine	OCH_3	C_2H_5	OH	CH_2OCH_3	OCH_3	$OCOCH_3$	OBz	OH	OH	645
Hypaconitine	OCH_3	CH_3	H	CH_2OCH_3	OCH_3	$OCOCH_3$	OBz	OH	OH	615
Benzoylaconitine	OCH_3	C_2H_5	OH	CH_2OCH_3	OCH_3	OH	OBz	OH	OH	603
Benzoylhypaconitine	OCH_3	CH_3	H	CH_2OCH_3	OCH_3	OH	OBz	OH	OH	573
Benzoylmesaconitine	OCH_3	CH_3	OH	CH_2OCH_3	OCH_3	OH	OBz	OH	OH	589
Neoline	OH	C_2H_5	H	CH_2OCH_3	OCH_3	OH	OH	H	H	437
Talatisamine	OCH_3	C_2H_5	H	CH_2OCH_3	H	OH	OH	H	H	421
Yunaconitine	OCH_3	C_2H_5	OH	CH_2OCH_3	OCH_3	$OCOCH_3$	$OBzOCH_3$	OH	H	659
Lappaconite Hydrobromide	OCH_3	C_2H_5	H	$OBzNHCOCH_3$	H	OH	OCH_3	H	H	584

Fig.1

Loading phase

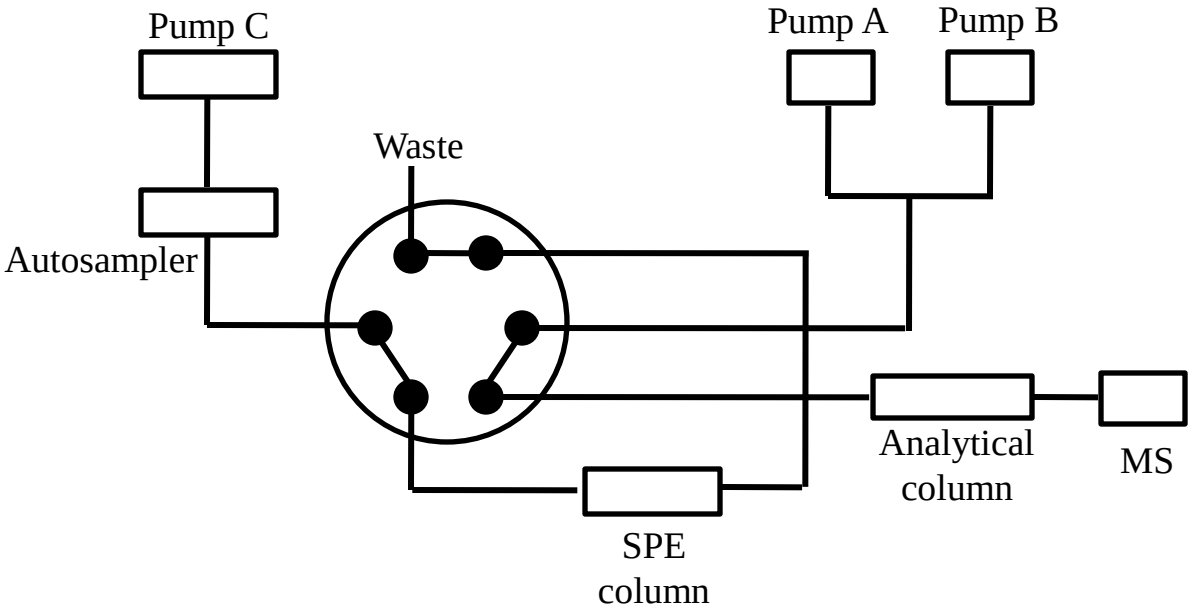

Elution phase

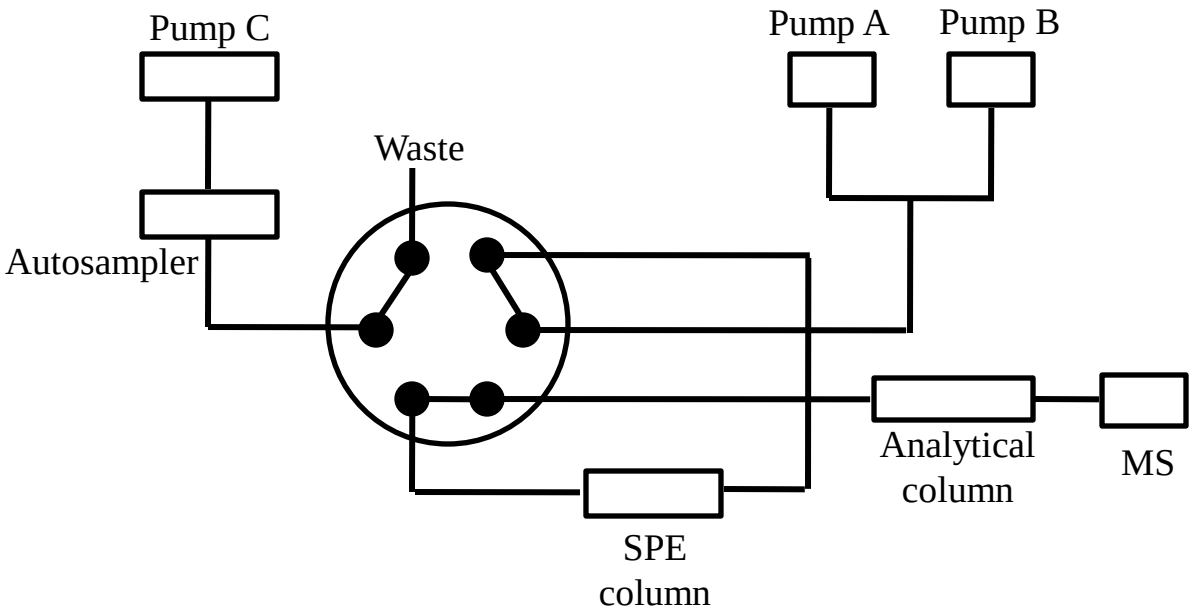

Fig. 2

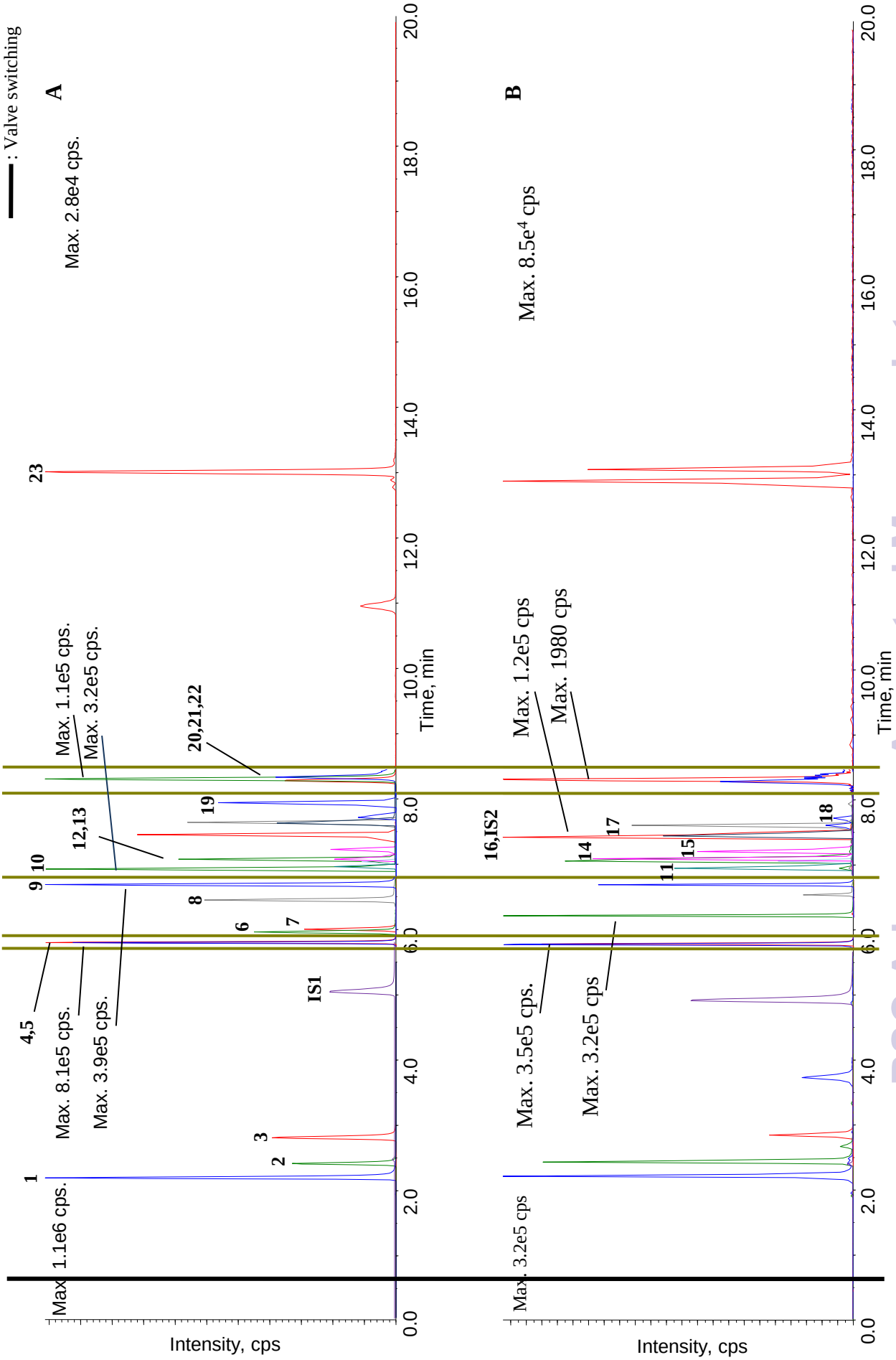

Fig.3